



**HAL**  
open science

## Low-Density Plastic Debris Dispersion beneath the Mediterranean Sea Surface

Alberto Baudena, Rainer Kiko, Isabel Jalón-Rojas, Maria Luiza Pedrotti

► **To cite this version:**

Alberto Baudena, Rainer Kiko, Isabel Jalón-Rojas, Maria Luiza Pedrotti. Low-Density Plastic Debris Dispersion beneath the Mediterranean Sea Surface. *Environmental Science and Technology*, 2023, 10.1021/acs.est.2c08873 . hal-04087301

**HAL Id: hal-04087301**

**<https://hal.sorbonne-universite.fr/hal-04087301>**

Submitted on 10 May 2023

**HAL** is a multi-disciplinary open access archive for the deposit and dissemination of scientific research documents, whether they are published or not. The documents may come from teaching and research institutions in France or abroad, or from public or private research centers.

L'archive ouverte pluridisciplinaire **HAL**, est destinée au dépôt et à la diffusion de documents scientifiques de niveau recherche, publiés ou non, émanant des établissements d'enseignement et de recherche français ou étrangers, des laboratoires publics ou privés.

Copyright

1 *Low-density plastic debris dispersion beneath*  
2 *the Mediterranean Sea surface*

3 Alberto Baudena<sup>1,\*</sup> Rainer Kiko<sup>1,2</sup> Isabel Jalón-Rojas<sup>3</sup>  
4 Maria Luiza Pedrotti <sup>1</sup>

5 <sup>1</sup>Sorbonne Université, CNRS, Laboratoire d’Océanographie de Villefranche,  
6 UMR 7093 LOV, Villefranche-sur-Mer, France

7 <sup>2</sup> GEOMAR Helmholtz Center for Ocean Research Kiel, Germany

8 <sup>3</sup>CNRS, UMR5805 EPOC, University of Bordeaux, 33615 Pessac, France

9 \*To whom correspondence should be addressed;

10 E-mail: alberto.baudena@gmail.com.

11 **Abstract**

12 Plastic is a widespread marine pollutant, with most studies focusing  
13 on the distribution of floating plastic debris at the sea surface. Recent evi-  
14 dence, however, indicates a significant presence of such low density plastic  
15 in the water column and at the seafloor, but information on its origin and  
16 dispersion is lacking. Here, we studied the pathways and fate of sinking  
17 plastic debris in the Mediterranean Sea, one of the most polluted world  
18 seas. We used a recent Lagrangian plastic-tracking model, forced with  
19 realistic parameters, including a maximum estimated sinking speed of 7.8  
20 m/d. Our simulations showed that the locations where particles left the  
21 surface differed significantly from those where they reached the seafloor,  
22 with lateral transport distances between 119–282 km. Furthermore, 60%  
23 of particles deposited on the bottom coastal strip (20 km wide) were re-  
24 leased from vessels, 20% from the facing country, and 20% from other  
25 countries. Theoretical considerations furthermore suggested that biological  
26 activities potentially responsible for the sinking of low density plastic  
27 occur throughout the water column. Our findings indicate that the res-  
28 sponsibility for seafloor plastic pollution is shared among Mediterranean  
29 countries, with potential impact on pelagic and benthic biota.

30 **Keywords:** low-density plastic, marine pollution, water column, seafloor, trans-  
31 port, sinking speed

32 **Synopsis:** Minimal information is available on the fate of plastics sinking from  
33 sea surface. Here we show that they potentially travel hundreds of km and that  
34 accountability for seafloor pollution is shared among Mediterranean countries.

35 **1 Introduction**

36 Plastic pollution represents a major threat to the oceans, causing socio-economic  
37 damage and impacting tourism, fishing, and marine ecosystems (1, 2). More  
38 than 914 marine species have been reported to accidentally ingest or be en-  
39 tangled by plastic, a number expected to increase in the near future (3). In

40 addition, plastic debris is a vector for invasive species and persistent organic  
41 pollutants (4, 5, 6). Around 300,000 metric tons of plastic have been estimated  
42 to float at the sea surface (7). However, they only represent a tiny portion of the  
43 plastic expected to enter the marine environment each year (8, 9, 10), suggest-  
44 ing that plastic may be even more present in other ocean compartments. Even  
45 if the amount of plastic entering the oceans (e.g., via rivers) and the plastic  
46 budget are still open questions (10, 11, 12), a growing body of evidence suggests  
47 that plastic debris is present not only at the sea surface, but in the whole water  
48 column and sea bottom (e.g. refs. 13, 14, 15, 16, 17, 18). Surprisingly, observa-  
49 tions reported plastic debris composed of polymers lighter than seawater in the  
50 water column, down to at least 1000 m depth (14).

51 Several processes are responsible for the removal of plastic debris from the sea  
52 surface, the most studied being biofouling (19, 20) - the colonisation of plastic  
53 debris by bacteria, algae or invertebrates - which increases its relative density.  
54 This process continues until, eventually, the debris leaves the surface, and has  
55 been documented by laboratory and, recently, by in situ studies (21, 22, 23, 24).  
56 Other processes that could lead to the removal of surface plastic debris are ag-  
57 gregation in marine snow and faecal pellet formation after ingestion (25, 26).  
58 However, information about the pathways and fate of settling plastic debris is  
59 lacking. A common assumption is that plastic debris reaches the seafloor where  
60 it has left the surface (27). This assumption has also been used to estimate the  
61 seafloor plastic concentration (16).

62 The aim of this study is to assess the validity of this assumption and to im-  
63 prove the understanding of plastic transport from the sea surface to the sea  
64 bottom. This information is essential to solve the plastic budget problem, to  
65 understand plastic fate, and for mitigation strategies. For that purpose, we use a  
66 Lagrangian plastic-tracking model to analyse (i) the potential pathways of plas-  
67 tic debris from the surface to the seafloor, (ii) its distribution once it reaches  
68 the seafloor, and (iii) its potential sources. We focus on plastic whose absolute  
69 density is lighter than seawater (referred to as low-density plastic, LDP), usually  
70 smaller than 5 mm in size (28). This includes low- and high-density polyethy-  
71 lene and polypropylene, which represent 88% of the LDP debris floating at the  
72 surface of the Mediterranean Sea (29), and about half of the produced plastic  
73 globally (30, 6). We only focus on the sinking phase of LDP debris, as multiple  
74 works already studied its cycle from the moment it is released at sea until it  
75 starts sinking (e.g. (31, 27, 32)). We do not consider high density plastic de-  
76 bris, which is expected to sink directly to the seafloor (17, 33) and about which  
77 there is little information, nor extremely light items which mainly float at the  
78 air-sea interface. Lagrangian methods are widely used to describe the transport  
79 of particles in the ocean and are suited to describe the transport of LDP debris.  
80 These models can cover areas wider than observations and can describe forward  
81 and backward trajectories useful to identify sources and pathways.

82 This study is a first modeling effort to evaluate the transport dynamics and fate  
83 of LDP in the Mediterranean Sea, which is an ideal case study for two main  
84 reasons: (i) globally, it is one of the most plastic polluted seas (28, 34); (ii)  
85 its plastic pollution at the sea surface has been intensively studied, allowing us  
86 to estimate key physical parameters such as plastic debris sinking speed and to  
87 set initial conditions. In particular, we combine recent observations of plastic  
88 concentration in the water column, the largest Mediterranean Sea database of  
89 floating LDP debris to date, one of the best performing drag models, and esti-

90 mates of the location and amount of LDP leaving the sea surface. The latter  
91 metric was obtained from the first Lagrangian model quantitatively validated in  
92 the Mediterranean Sea (31), by assuming that the probability of a LDP leaving  
93 the surface increases with the time it spent in water according to a prescribed  
94 function. With this information, we are also able to calibrate the model and  
95 perform a detailed sensitivity test. We then provide an assessment of the paths  
96 and fate of LDP sinking in the Mediterranean sea as well as an estimation of  
97 the contribution of the different countries to the coastal seafloor pollution. Fi-  
98 nally, we consider the implications of the calculated density differences between  
99 generic sinking LDP debris and seawater to assess the role of biological transport  
100 throughout the water column, consistent with recent studies.

## 101 2 Materials and Methods

### 102 2.1 The numerical Lagrangian model: velocity field and 103 trajectory computation

104 Here, we simulate the path of LDP debris once they start sinking from the sur-  
105 face (due to biofouling or other processes) down to 1000 m. We do not analyse  
106 what occurs to debris prior to that (i.e., from the moment it was released at  
107 sea to when it left the sea surface), as several studies already investigated this  
108 question (e.g. (31, 27, 35)). Hence, this study can be seen as a continuation  
109 of those works. To this aim, we used the TrackMPD model (36), an advanced  
110 3D Lagrangian model recently developed to simulate the fate of plastic debris  
111 at sea. The TrackMPD model reads the velocity field offline, and computes the  
112 trajectories with a Runge-Kutta scheme of order 4-5 both in time and space.  
113 Time steps were set to 3 hours. Model initialisation and simulated scenarios are  
114 reported in Subsec. 2.3.

115 The velocity field used to simulate the virtual particle trajectories was a high  
116 resolution configuration of the NEMO model (NemoMed36;  $1/36^\circ \times 1/36^\circ$ ) pro-  
117 vided at daily intervals, with 50 stretched vertical levels (sigma coordinate sys-  
118 tem), developed by Arsouze et al. (37). This circulation model was initialised  
119 with sea surface temperature and salinity fields and took into account riverine  
120 freshwater runoff. It included the vertical component of the velocity field  $w$  as  
121 well. This product has already been used to simulate 3D virtual plastic trajec-  
122 tories in the Mediterranean Sea (38).

123 A Stokes component was added to the NemoMed36 velocity field. The Stokes  
124 product (MEDSEA\_HINDCAST\_WAV\_006.012), with a spatial resolution of  
125  $1/24^\circ$ , was spatially interpolated over the grid of NemoMed36, and was summed  
126 to its upper layer. This allowed us to take into account Stokes drift due to waves  
127 at the surface, which affects particles in the first meters of their sinking. Stokes  
128 effect indirectly includes windage and is known to affect plastic fate (39).

### 129 2.2 Constraining the model settings

130 A key parameter to study the fate of (biofouled) sinking LDP debris in the  
131 water column is its settling speed. In situ observations of LDP settling speed  
132 are not available to date. A few studies have measured the settling velocity of  
133 biofouled plastic particles under laboratory conditions and found that a large  
134

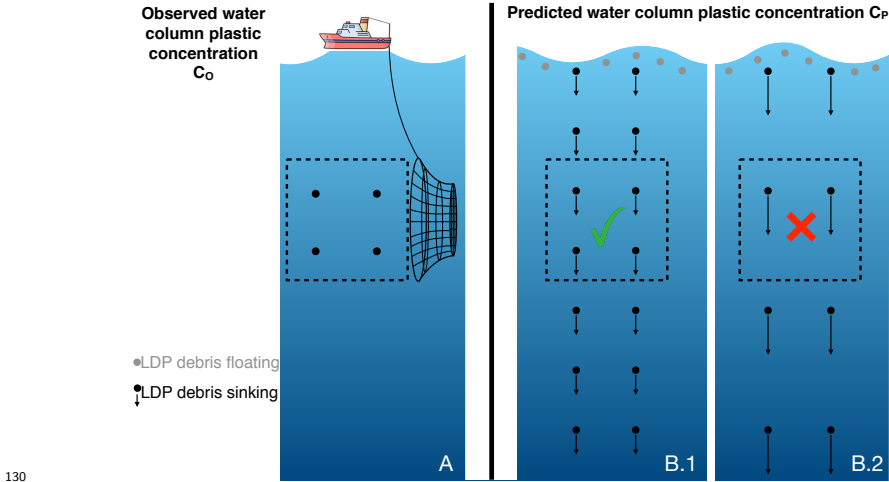


Figure 1: Illustrative scheme of the paradigm used to calculate the sinking speed of LDP debris. The predicted water column LDP concentration  $C_P$  decreases when LDP sinking speed increases (panels B.1 and B.2). In order to have  $C_P$  equal or greater to a given value observed  $C_O$  (panel A), the LDP sinking speed must not be larger than a given value. In this case panel B.1 represents the maximum possible sinking speed of LDP debris. Panel B.2 shows that, if a larger sinking speed is considered, then  $C_P$  is lower than  $C_O$ .

number of parameters, both physical (e.g. particle polymer, shape and size; water temperature and salinity) and biological (e.g. biofilm growth and density) can impact the sinking speed (33, 24, 19). The large spectrum of sinking LDP and environmental conditions in the ocean make difficult the definition of settling speed in numerical simulations. For these reasons, we calculated a (maximum) representative sinking speed value to calibrate our model, ensuring that mean simulated and observed LDP concentrations in the water column have the same order of magnitude. We assumed that the water column LDP concentration is the result of a linear fall of LDP debris from the sea surface. The larger the LDP sinking speed, the lower the water column LDP concentration for a given rate of plastic submergence from surface (Fig. 1). By taking the lowest water column LDP concentration measured to date as the lower boundary, we can derive a maximum sinking speed, which will be the reference value in the simulations. Details of the calculation are provided in the following subsections. The choice of a linear fall of LDP debris is evaluated by integrating the largest LDP database in the Mediterranean Sea to date ( $\sim 75,000$  debris) and with a drag model (Subsec. 2.5).

### 2.2.1 Observed water column plastic concentrations $C_O$

Here, we report the current literature on observed plastic concentrations in the ocean water column (hereafter  $C_O$ ) in Table 1 (adapted from Liu et al., (40)) which is used to calibrate the simulated plastic concentration in the model. We did not consider the measurements sampled at a depth shallower than 50 m to exclude mixing layer processes, except for the study of Lattin et al., (41), as it is

166 among the only 4 studies which measured the LDP mass concentration ( $\mu\text{g}/\text{m}^3$ )  
167 to date. The highest concentrations were measured by Pabortsava et al., (42)  
168 ( $940 \mu\text{g}/\text{m}^3$ ) and Lattin et al., (41) ( $150 \mu\text{g}/\text{m}^3$ ), the lowest by Egger et al.,  
169 (14) ( $1.6 \mu\text{g}/\text{m}^3$ , averaged on the 5–1000 m depth layer).  
170 Four studies measured  $C_O$  in coastal areas of the Mediterranean Sea (43, 15,  
171 44, 45). Bainsi et al., (43) and Lefebvre et al., (15) found similar concentrations  
172 ( $0.23 \pm 0.20 \text{ particles}/\text{m}^3$ ;  $0.26 \pm 0.33 \text{ particles}/\text{m}^3$ , respectively). Vasilopoulou et  
173 al., (44) and Rios-Fuster et al., (45), sampling in shallower waters ( $< 50 \text{ m}$ ), and  
174 close to the coast, found water column plastic concentration  $\sim 200$  times larger  
175 ( $41 \pm 22$  and  $67 \pm 52 \text{ particles}/\text{m}^3$ , respectively). Interestingly, Rios-Fuster et al.,  
176 (45) found LDP debris down to 50 m depth.  
177 As the studies on the Mediterranean Sea did not measure the mass of plastic  
178 debris, we compared them with the concentrations of Egger et al., (14) which  
179 reported the lowest concentrations in  $\mu\text{g}/\text{m}^3$  and  $\text{particles}/\text{m}^3$  and can serve as a  
180 reference value of minimum plastic concentration in the water column to obtain  
181 in our simulations. Egger et al., (14) collected LDP debris larger than  $500 \mu\text{m}$ ,  
182 76% of plastic debris collected by Bainsi et al., (43) was larger than  $500 \mu\text{m}$ , while  
183 the mean size of plastic debris found by Lefebvre et al., (15) was ( $1.81 \pm 1.42$ )  
184 mm, indicating that most of debris was larger than  $500 \mu\text{m}$ . Therefore, Egger  
185 et al., (14), Bainsi et al., (43), and Lefebvre et al., (15) studies collected plastic  
186 debris of similar size range, but the concentration measured by Egger et al.,  
187 (14) was  $\sim 200$  times lower ( $0.001 \text{ particles}/\text{m}^3$ ). Hence, Mediterranean water  
188 column plastic concentrations are probably larger than those measured by Egger  
189 et al., (14) also when considering the mass ( $\mu\text{g}/\text{m}^3$ ). This is also corroborated  
190 by the fact that the Mediterranean is one of the seas most affected by plastic  
191 pollution, with surface LDP concentrations comparable to those found in the  
192 North Pacific Garbage Patch (NPGP) (28, 34, 43). Biofouling was predicted to  
193 be larger in several regions of the Mediterranean Sea than in the oligotrophic  
194 NPGP area (32), suggesting that more LDP particles might leave the surface  
195 in the Mediterranean. However Mediterranean Sea studies (43, 15, 44) sampled  
196 lower water volumes, inducing possible biases towards higher concentrations (46,  
197 40, 47). Therefore, we considered a minimum water column LDP concentration  
198  $C_{O_{MIN}} = 1.60 \mu\text{g}/\text{m}^3$

Sampling regions	Methods	Samples pretreatment and polymer analysis	Volume/sample (L)	Depth (m)	Mesh size of nets <sup>a</sup> or filters (sieves) <sup>b</sup> (µm)	MP's size (mm)	Plastic concentration (items/m <sup>3</sup> )	Plastic concentration (µg/m <sup>3</sup> )
Arctic Central Basin (Kashai et al., 2018, ref. 48)	CTD sampler	Direct filtration; µ-FIR spectrometer	7-48	8-1370	250 <sup>a</sup> ; 120 <sup>b</sup>	0.25-5.00	0-100	/
Mariana Trench (Peng et al., 2018, ref. 49)	CTD sampler	Direct filtration; Raman spectroscopy	35-180	2,673-10,904	0.22 <sup>b</sup> ; 0.30 <sup>b</sup>	1.00-3.00 (mostly) <sup>c</sup>	(2-14)·10 <sup>6</sup>	/
Baltic Sea proper (Buguev et al., 2017, ref. 50)	CTD sampler	Direct filtration; Combination of visual identification and UV lamp	7.79-30	0.5-217.5	174 <sup>b</sup>	N/A <sup>d</sup>	80 (fibers)	/
Sumba coastal waters, Indonesia (Cordova et al., 2018, ref. 51)	CTD sampler	Direct filtration; FIR spectrometer	10	5-300	0.45 <sup>b</sup>	0.30-1.00 (mostly) <sup>c</sup>	44±25	/
Baltic Sea, Sweden (Gorokhova, 2015, ref. 52)	Plankton net	Direct observation; visual identification	6,200-9,200	0-100	90 <sup>a</sup>	0.05-0.30 (mostly) <sup>c</sup>	2000-3000	/
Tuscany coastal waters, Mediterranean Sea (Zhu et al., 2018, ref. 43)	Plankton net	Direct observation; FIR spectrometer	500-30,000	2-120	200 <sup>a</sup>	1-2.5 (mostly) <sup>c</sup>	0.26	/
Gulf of Lions (Leclercq et al., 2019, ref. 15)	Plankton net	Direct observation; FIR spectrometer	N/A <sup>d</sup>	0-100	200 <sup>a</sup>	0.24-4.93	0.23±0.20	/
Cyprus coasts (Vassilopoulou et al., 2021, ref. 44)	Plankton net	Direct observation; DMIL microscope and SLX-3 stereoscope	N/A <sup>d</sup>	0-50	200 <sup>a</sup>	0.2-5	41.31±22.41	/
Spanish coast (Rios-Fuster et al., 2022, ref. 45)	Niskin bottles	Direct filtration; FIR spectrometer on 10% of items	5	5-50	1.2 <sup>b</sup>	0.1-8.4	1860±1430 (67 without fibers)	/
Northeast Pacific (Goldstein et al., 2013, ref. 53)	Plankton net	Direct observation; FIR spectrometer	N/A <sup>d</sup>	0-210	202 <sup>a</sup>	N/A <sup>d</sup>	0.05	/
Santa Monica Bay (Lain et al., 2004, ref. 41)	Multi-net trawls	Freshwater floatation; No polymeric identification	N/A <sup>d</sup>	0-14.80	333 <sup>a</sup>	2.80-4.75 (mostly) <sup>c</sup>	/	150
North Pacific Garbage Patch (Egger et al., 2020, ref. 14)	Multiple Opening and Closing Net	Direct observation; Raman spectroscopy	136,000-5,039,000	0-2,003	333 <sup>a</sup> ; 500-15,000 <sup>b</sup>	N/A <sup>d</sup>	0.001	1.60
Baltic Sea, Russia (Zubkov et al., 2019, ref. 54)	Submersible pump	Organics removal prior to the refiltration (174µm); µ-Raman spectroscopy	2,500-3,500	0.5-91	174 <sup>b</sup>	0.17-1.00 (mostly) <sup>c</sup>	32	/
Korean coastal waters (Song et al., 2018, ref. 55)	Submersible pump	NaCl solution floatation prior to the refiltration; µ-FIR spectrometer	100	3-58	20 <sup>b</sup> ; 5 <sup>b</sup>	0.02-5.00	423 (50 if only particles < 5 mm)	/
Monterey Bay (Choi et al., 2019, ref. 13)	In-situ filtration device	Direct observation; Raman spectroscopy	1,007-2,378	5-1,001	100 <sup>b</sup>	N/A <sup>d</sup>	1-10	/
HAUSGARTEN observatory (Rikman et al., 2020, ref. 56)	In-situ filtration device	Organics removal prior to the filtration; µ-FIR spectrometer	218-561	1-5,351	32 <sup>b</sup>	0.01-0.15	95±85	/
West Pacific and East Indian Ocean (Li et al., 2020, ref. 47)	In-situ filtration device	Wet peroxide oxidation; µ-FIR spectrometer	10,000	2-4001	60 <sup>b</sup> ; 1.60 <sup>b</sup>	0.03-6.33 (mean 0.07)	0.2-3.5	/
Atlantic Ocean (Fabrisova et al., 2020, ref. 42)	In-situ filtration device	Organics removal prior to the filtration; µ-FIR spectrometer	500-1500	0-201	55; 25	0.032-0.651	2300	940
Atlantic Ocean (Zhao et al., 2022, ref. 57)	Multiple Opening and Closing Net; WTS-LV pump	Direct observation; visual identification; µ-FIR spectrometer	440-1765	0-5200	200 <sup>a</sup>	SMP: <100µm; LMP: >300µm	SMP: 0.244.3; LMP: 0.0011	SMP: 0.20.83; LMP: 0.15.3

a. mesh size of net used in the reference.  
b. mesh size of filter or sieve used in filtering process.  
c. only size range of MPs was presented in the literature.  
d. N/A represented no available information.

Table 1: Literature on Mediterranean water column plastic concentration (adapted with permission from Liu et al., (40), Copyright 2020 Elsevier).

203 **2.2.2 Annual estimates of LDP plastic entering the Mediterranean**  
 204 **Sea.**

205 We defined  $N_{TBY}$  as the number of tons of LDP leaving the Mediterranean  
 206 surface every year due to biofouling or other processes.  $N_{TBY}$  was obtained  
 207 assuming that  $\sim 11.5\%$  of the amount of floating plastic debris entering the  
 208 Mediterranean Sea every year from coastal sources or vessel discards ( $N_{LDPY}$ )  
 209 left the sea surface during that period due to biofouling or other processes. This  
 210 percentage was based on the study by Baudena et al., (31), and was similar to  
 211 the value obtained in a previous study (9.2 %, 27). Thus:

$$N_{TBY} = 0.115 \cdot N_{LDPY} . \quad (1)$$

212  $N_{LDPY}$  was estimated using the findings of ref. (8). The authors calculated the  
 213 number of tons of plastic debris entering the global ocean in 2010. Considering  
 214 that  $\sim 50\%$  of plastic is LDP (mainly low- and high-density polyethylene and  
 215 polypropylene, 30, 6), about 100,000 tons of LDP debris were estimated to enter  
 216 the Mediterranean Sea in 2010. This quantity includes also extremely light and  
 217 large LDP not considered here. However, these constitute less than 1% of items  
 218 collected in the Mediterranean Sea (28). Overall, the assumed quantity repre-  
 219 sents a compromise between recent estimates, both lower (58, 59) and higher  
 220 (11, 10). Furthermore, we stress that this value was adopted in recent studies  
 221 modelling plastic-debris dispersion in this basin (27, 38, 31). The sensitivity  
 222 of the results with respect to this parameter is studied by simulating a further  
 223 scenario (Subsec. 2.3).  
 224

225 **2.2.3 Estimation of the maximum sinking speed of LDP debris  $SS_{MAX}$**

226  $N_{TBY}$  can be converted into a flux  $F$  of LDP mass leaving each  $m^2$  of sea surface  
 227 every day by considering the Mediterranean surface ( $\simeq 2.5 \times 10^{12} m^2$ ):

$$F = \frac{N_{TBY} \cdot 10^6}{365 \cdot 2.5 \cdot 10^{12}} \frac{g}{dm^2} = 1.10 \cdot 10^{-9} N_{TBY} \frac{g}{dm^2} \quad (2)$$

228 The predicted concentration of the falling particles in the water column  $C_P$   
 229 (expressed as  $g/m^3$ ) depends on their vertical sinking velocity  $SS$ . We stress  
 230 that the flux of particles sinking from the sea surface is a release of individual  
 231 particles (the LDP debris) at discrete intervals (Fig. 1), similar to a *rain effect*.  
 232 Thus, the concentration  $C_P$  was considered as the ratio between  $F$  (Expr. 2)  
 233 and  $SS$  (expressed in m/d, Fig. 1):

$$C_P = \frac{F}{SS} = \frac{N_{TBY}}{SS} 1.10 \cdot 10^{-9} \frac{g}{m^3} \quad (3)$$

234 Expr. (3) implies that the more slowly LDP debris sinks, the greater the re-  
 235 sulting water column plastic concentration is, and vice versa (Fig. 1, panels B.1  
 236 and B.2). If  $N_{TBY}$  increases (and we assume the same sinking speed), so does  
 237 the water column plastic concentration. Here,  $C_P$  was derived considering the



238 same sinking speed and mass for all the particles. We also derived an expres-  
 239 sion for the predicted concentration by considering individual sinking speed and  
 240 mass, and showed that these did not affect  $C_P$ , nor the conclusions of our paper  
 241 (Supporting Information S.1).

242 By inverting Expr. (3), we could obtain an expression for the sinking speed of  
 243 the LDP debris,  $SS$ :

$$SS = \frac{N_{TBY}}{C_P} 1.10 \cdot 10^{-9}, \quad (4)$$

244 from which it was possible to obtain a maximum estimate of the settling speed  
 245  $SS_{MAX}$  in the Mediterranean Sea. To do so, we considered the estimate of  
 246  $N_{TBY}$  for the Mediterranean Sea (11,500 tons/year, Subsec. 2.2.2) and imposed  
 247  $C_P=C_{O_{MIN}}$  ( $1.60 \mu\text{g}/\text{m}^3$ , Egger et al., (14), Subsec. 2.2.1):

$$SS_{MAX} = \frac{N_{TBY}}{C_{O_{MIN}}} 1.10 \cdot 10^{-9}, \quad (5)$$

248 By substituting these values in Expr. (5), we obtained  $SS_{MAX}=7.8$  m/d.

249 In summary, in order to have a minimum water column plastic concentration  
 250 of  $1.60 \mu\text{g}/\text{m}^3$ , considering a maximum load of 11,500 tons of biofouled LDP  
 251 leaving the surface each year, LDP debris should sink with a maximum settling  
 252 speed of 7.8 m/d. Considering a greater water column plastic concentration,  
 253 and/or a lower load of biofouled LDP per year would lead to a lower sinking  
 254 speed.

255 We stress that using the  $C_O$  values of Baini et al., Lefebvre et al., Vasilopoulou et  
 256 al., (43, 15, 44) (converted in plastic mass) as  $C_{O_{MIN}}$  rather than those of Egger  
 257 et al., (14),  $SS_{MAX}$  would have been lower. Similarly, using a lower  $N_{LDPY}$  (and  
 258 thus a lower  $N_{TBY}$ ) would have lead to a lower  $SS_{MAX}$  value. Nevertheless,  
 259 we considered a two fold value of  $N_{TBY}$ , by carrying out a simulation with a  
 260 sinking speed set to twice  $SS_{MAX}$  (15.6 m/d, Subsec. 2.3).

### 261 **2.3 Model initialisation and simulated scenarios**

265 The simulated particles were considered representative of LDP debris of all sizes,  
 266 with the exception of extremely light foamed plastics (such as polystyrene foam)  
 267 or air filled objects which tend to stay suspended at the air-sea interface. The  
 268 latter represent less than 1% of plastic debris collected in the Mediterranean  
 269 Sea (28). In general, 95% of LDP debris collected in the Mediterranean Sea  
 270 are less than 5 mm in size (28). LDP debris were considered to sink, assuming  
 271 that biofouling, weathering or other processes decrease the buoyancy of these  
 272 particles. Virtual LDP particles were released at the surface at daily intervals  
 273 between January 1, and December 31, 2010. This time interval is consistent  
 274 with the residence time of plastic debris at the Mediterranean surface (31, 27).  
 275 To initialise the particle starting positions, we used the results of Baudena et  
 276 al., (31), which simulated the path of LDP debris from their release at sea (by  
 277 coastal cities, river mouths, and vessels) to the moment they started sinking.  
 278 In that work, the authors assumed that the probability of a simulated LDP  
 279 particle leaving the sea surface (due to e.g. biofouling, etc.) increases with  
 280 the time spent in water. This probability peaked in correspondence with the

281 biofouling time (the period of time necessary to induce sinking, see Supplemen-  
282 tary Fig. 2 in Baudena et al., 31). In this way, the authors calculated the  
283 Mediterranean surface sinking rate (the amount of LDP debris that disappears  
284 from the surface each day in a square kilometer of sea surface). To strengthen  
285 that metric Baudena et al., (31) considered different biofouling times (between  
286 50–200 days, based on literature values) and obtained similar estimates when  
287 considering 16 different parameterisations and an ensemble average. Hence, in  
288 our study, particles were released proportionally to the Mediterranean surface  
289 sinking rate, i.e. the larger the surface sinking rate in a region, the larger the  
290 number of particles released there. The choice of the dataset of Baudena et  
291 al.(31) is further motivated by the fact that it was the first Lagrangian model  
292 quantitatively validated in the Mediterranean Sea.

293 7,652,197 virtual particles were released in total, using four sinking speed values  
294 (7.8 m/d, Scenario 1; 4 m/d, Scenario 2; 2 m/d, Scenario 3; 1 m/d, Scenario  
295 4; Table 2). The choice of the maximum value used for the sinking speed  
296 ( $SS_{MAX}=7.8$  m/d) is motivated in Subsec. 2.2. All virtual plastic particles  
297 of a given scenario were advected for a time period (provided in Table 2) long  
298 enough to reach at least 1000 m depth. For scenario 4 (sinking speed of 1 m/d),  
299 particles were advected for 1000 days. At the end of the simulation, 90% of  
300 particles reached 1000 m depth or were deposited. The 10 % left were at an  
301 average depth of  $900\pm 100$  m, thus very close to reaching 1000 m depth. Thus,  
302 we use their final position to calculate the seafloor concentration (Subsec. 2.4).  
303 The particles were considered as non-inertial passive tracers with a constant  
304 sinking velocity, which were transported by currents and by isotropic horizontal  
305 and vertical diffusion (diffusivity coefficient  $K_h$  and  $K_v$ , respectively).

306 We used  $K_h=10$  m<sup>2</sup>/s and  $K_v=5\cdot 10^{-5}$  m<sup>2</sup>/s, in line with the values used in pre-  
307 vious plastic studies (27, 36, 58, 31). In order to test the sensitivity of the results  
308 to the choice of the diffusivity coefficients, different  $K_h$  and  $K_v$  values were used  
309 (Scenarios 5–8, Table 2). In order to evaluate the role of the vertical component  
310 of the current field  $w$  on the simulated LDP concentration,  $w$  was set to zero  
311 in scenario 9 (Table 2). Scenarios 5–9 were run with the same sinking speed of  
312 Scenario 1, namely 7.8 m/d. In order to evaluate the sensitivity of the results  
313 with respect to a potentially larger  $SS_{MAX}$  (which could be due to a larger flux  
314 of LDP leaving the surface, Subsec. 2.2.3), in Scenario 10 we used a sinking  
315 speed of 15.6 m/d. Finally, in Scenario 11 we evaluated the sensitivity of the  
316 results with respect to the release conditions: to do so, the surface sinking rate  
317 of Baudena et al. (31) was varied at each location of  $\pm 10\%$  randomly. This new  
318 sinking rate was used to initialise the particle release locations of that scenario.

319

## 320 2.4 Model output analyses

321 One of the limitations in simulating particle trajectories from the surface to the  
322 seafloor in a deep basin such as the Mediterranean Sea is the elevated compu-  
323 tational cost. To overcome this issue, we calculated the concentration of the  
324 simulated particles on a virtual layer at 1000 m depth. In the regions with a  
325 seafloor shallower than 1000 m, we kept the original depth (provided by the ve-  
326 locity field domain (37)). 1000 m was chosen as the reference depth because it is  
327 usually considered as the upper boundary of the deep sea. Thus, LDP reaching  
328 this layer are therefore considered as sequestered in the deep sea. Furthermore,

N° Scenario	Current velocity field	Vertical component of currents included (yes/no)	Sinking speed particles (m/d)	Release period	Advective period (days)	$K_h$ (m <sup>2</sup> /s)	$K_v$ (m <sup>2</sup> /s)	Notes
S1	NemoMed36	yes	7,8	1 Jan-31 Dec 2010	450	10	$5 \cdot 10^{-5}$	
S2	NemoMed36	yes	4,0		550			
S3	NemoMed36	yes	2,0		1050			
S4	NemoMed36	yes	1,0		1050			
S5	NemoMed36	yes	7,8		450	5	$5 \cdot 10^{-5}$	
S6	NemoMed36	yes	7,8		450	15		
S7	NemoMed36	yes	7,8		450	10	$1 \cdot 10^{-5}$	
S8	NemoMed36	yes	7,8		450		$10 \cdot 10^{-5}$	
S9	NemoMed36	no	7,8		450	10	$5 \cdot 10^{-5}$	
S10	NemoMed36	yes	15,6		225	10	$5 \cdot 10^{-5}$	
S11	NemoMed36	yes	7,8		450	10	$5 \cdot 10^{-5}$	

262

264

Table 2: Parameters used for each of the ten simulated scenarios.

329 this assumption allowed us to simulate sinking speeds down to 1.0 m/d, which  
330 would not have been possible for further depths due to computational costs.  
331 The concentration on a deeper virtual seafloor, at 2000 m depth, was calculated  
332 for scenarios 1–3 only, and is reported in Supporting Information S.2.

333 Further, we calculated the concentration of particles deposited less than 20 km  
334 from the coast (hereafter the coastal strip). We chose this distance because it is  
335 associated with the inner average continental shelf, exploited by industrial and  
336 recreational fishery and essential for tourism activity (60, 61). This concentra-  
337 tion was calculated for each Mediterranean country. For each deposited particle  
338 we identified if it was released by a land (coastal city or river mouth) or a sea  
339 (vessel discard) source. To this aim, we tracked each particle backward in time  
340 from the seafloor to the surface (using our trajectories) and from the surface to  
341 its release source (using the trajectories calculated by Baudena et al., 31). If the  
342 original release source was land based, we determined the corresponding source  
343 country as well. The plastic sources considered were those used in Baudena et  
344 al., (31), coastal cities (62), river mouths (63), and vessel discards (64).

345 We analysed the connectivity between Mediterranean surface and seafloor by  
346 considering the starting and final position of each particle and by calculating  
347 a connectivity matrix (65) at two different resolutions. Further details are re-  
348 ported in Supporting Information S.3.

349 To understand the pathways of the LDP particles reaching a zone of high LDP  
350 concentration, located north-east of the Balearic archipelago (Fig. 3A), we cal-  
351 culated their crossroadness (66, 31). This metric provides, for a given point, the  
352 percent of the trajectories that passed in its neighborhood (defined as a circle  
353 of radius  $0.1^\circ$ ). Further details are reported in Supporting Information S.4.

## 354 2.5 Density of sinking LDP debris from a drag model

355 In Subsec. 2.2.3, we estimated a maximum sinking speed  $SS_{MAX}$  of LDP debris  
356 equal to 7.8 m/d. Here we calculate the difference of LDP and seawater densities

357 necessary to obtain such value. To this aim we use (i) the largest LDP debris  
 358 dataset collected in the Mediterranean Sea to date and (ii) the drag model of  
 359 Dioguardi et al., (67).

360  
 361 **Mediterranean Sea LDP debris database**

362 We exploited the largest LDP field dataset in the Mediterranean Sea to date,  
 363 collected during the Tara Expedition (122 stations, ref. 28,  
 364 <https://zenodo.org/record/5538238>). This dataset provided the ferret (considered  
 365 representative of the particle size  $d_p$ ), sphericity  $\Phi$ , and circularity  $\chi$  of  
 366 each LDP debris collected at the sea surface (75,030 items in total). We used  
 367 these debris physical properties to estimate the velocity at which they are expected  
 368 to sink once biofouled.

369  
 370 **Drag model to calculate the sinking velocity**

371 Van Melkebeke et al., (68) evaluated eleven drag models estimating the vertical  
 372 sinking velocities of plastic particles with different characteristics, such as size,  
 373 shape, and density. The best performing drag model was the one reported in  
 374 (67, average error of 13.20%), which calculated the vertical sinking speed  $SS_{DM}$   
 375 as follows:

$$SS_{DM} = \sqrt{\frac{4gd_p\Delta\rho}{3C_d\rho_{SW}}}, \quad (6)$$

376 where  $g$  is the gravity acceleration (9.81 m/s<sup>2</sup>),  $d_p$  is the particle size,  $\Delta\rho$  is the  
 377 difference between the particle density and that of seawater,  $\rho_{SW}$ .  $C_d$  is the  
 378 particle drag coefficient, which the authors expressed as follows:

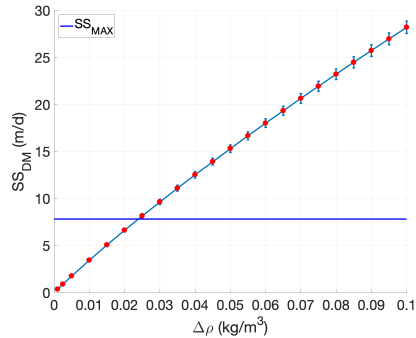
$$C_d = \frac{24}{Re_p} \left( \frac{1 - \Psi}{Re_p} + 1 \right)^{0.25} + \frac{24}{Re_p} (0.181 Re_p^{0.65}) \Psi^{-Re_p^{0.08}} + \frac{0.4251}{1 + \frac{6881}{Re_p} \Psi^{5.05}},$$

379 where  $Re_p$  is the particle Reynolds number.

$$Re_p = \frac{\rho_{SW} SS_{DM} d_p}{\mu_f},$$

380 with  $\mu_f$  being the water dynamic viscosity. The range of validity of Eq. (6)  
 381 is  $0.03 < Re_p < 10^4$ , which was respected with the parameters used.  $\Psi$  is the  
 382 shape factor, defined as the ratio between the particle sphericity  $\Phi$  and circularity  
 383  $\chi$ . The vertical sinking velocity  $SS_{DM}$  depends therefore on the six  
 384 parameters,  $d_p$ ,  $\Delta\rho$ ,  $\rho_{SW}$ ,  $\mu_f$ ,  $\Phi$ , and  $\chi$ . We considered a seawater density  
 385  $\rho_{SW}=1027$  kg/m<sup>3</sup> and a viscosity  $\mu_f=0.00109$  Pa·s; the latter is representative  
 386 of a seawater temperature of 20° ([https://www.engineeringtoolbox.com/seawater-properties-d\\_840.html](https://www.engineeringtoolbox.com/seawater-properties-d_840.html)), which is the mean Mediterranean surface temperature.  
 387 As  $d_p$ ,  $\Phi$ , and  $\chi$  we used the  $d_p$ ,  $\Phi$ , and  $\chi$  of each of the 75,030 debris  
 388 collected during the Tara expedition (Subsec. 2.5). Therefore,  $\Delta\rho$  represents  
 389 the only unknown parameter in Expr. 6.

390  
 391  
 392 Different  $\Delta\rho$  values were tested in Expr. (6), ranging from 0.001 to 0.1  
 393 kg/m<sup>3</sup>. The Matlab function provided in Dioguardi et al., (67) was used to  
 400



392

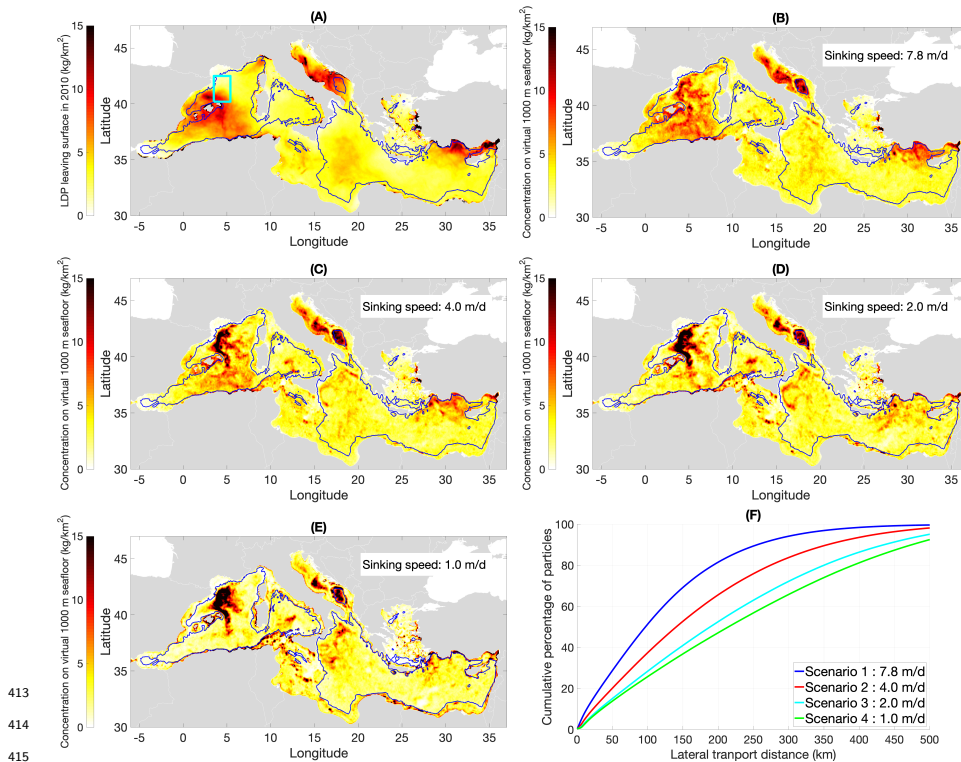
393 Figure 2: Mean theoretical sinking speed  $SS_{DM}$  of 75,030 LDP debris ( $y$ -axis,  
 394 subsec. 2.5) as a function of the difference between the density of the biofouled  
 395 LDP debris and the seawater  $\Delta\rho$  ( $x$ -axis).  $SS_{DM}$  are reported as mean values  
 396 (red dots) with standard deviation (errorbar). The blue horizontal line identifies  
 398 the  $SS_{MAX}$  value calculated in Subsec. 2.2.3 (7.8 m/d).

401 calculate 75,030  $SS$  values, which were then averaged together. We found that  
 402  $SS_{DM}$  matched  $SS_{MAX}$  for  $\Delta\rho \simeq 0.025 \text{ kg/m}^3$  (Fig. 2). The  $\Delta\rho$  obtained did  
 403 not change considerably when the predicted water column plastic concentration  
 404  $C_P$  was calculated considering also the individual mass of each of the 75,030  
 405 LDP debris (Supporting Information S.1). We also performed a sensitivity test  
 406 to analyse the robustness of the mean  $SS_{DM}$  while varying the three other  
 407 parameters  $d_p$ ,  $\rho_{SW}$ , and  $\mu_f$ . These calculations indicated that they did not  
 408 affect the mean  $SS_{DM}$  value (Supporting Information S.5) significantly.  
 409 Overall, above considerations show that only a minor excess density of 0.025  
 410  $\text{kg/m}^3$  compared to seawater is required to reach a maximum sinking speed of  
 411 7.8 m/d. Smaller  $\Delta\rho$  are related to lower sinking speeds.

### 412 3 Results

#### 430 3.1 Concentration of deposited LDP debris and distance 431 travelled during its sinking

441 The spatial distribution of particles deposited on the 1000 m depth virtual layer  
 442 (Fig. 3B, C, D, and E;) was consistently different from the distribution of  
 443 particles leaving the surface (Fig. 3A) for all the sinking speeds considered.  
 444 When reducing the sinking speed, the difference increased (Fig. 3B to Fig. 3E).  
 445 This result was particularly visible in the western Mediterranean: while large  
 446 amounts of virtual particles were predicted to leave the surface north of the  
 447 Balearic archipelago, the concentration at 1000 m depth in this same region  
 448 was relatively low for all the scenarios considered. Conversely, the 1000 m con-  
 449 centration was greater north-east of the Balearic archipelago, in a region where  
 450 the surface sinking rate was lower (cyan rectangle in Fig. 3A). This region,  
 451 covering 1.63% of the Mediterranean surface, contained 1.36% of the virtual  
 452 LDP particles leaving the Mediterranean surface. Notably, at 1000 m depth, it  
 453 accumulated the 3.07 %, 4.68%, 6.66%, and 7.36% of the virtual LDP particles  
 454 for scenarios 1–4, respectively. The LDP particles deposited there were mostly



416 Figure 3: **(A)**: amount of virtual LDP particles that left the Mediterranean  
 417 surface in 2010 (the surface sinking rate integrated between January 1, and  
 418 December 31, 2010; kg/km<sup>2</sup>; adapted with permission from Baudena et al.,  
 419 (31), Copyright 2022 Nature). **(B–E)**: concentration of virtual LDP particles  
 420 released in 2010 deposited on a virtual seafloor at 1000 m depth, for scenario 1,  
 421 2, 3, and 4, respectively. The virtual 1000 m seafloor was built by considering  
 422 all the seafloor locations deeper than 1000 m as 1000 m deep. The blue lines  
 423 in panel A–E indicate the 1000 m isobath. **(F)**: cumulative pdf of the lateral  
 424 transport distance (the distance between the location in which the particle left  
 425 the surface and the location in which it reached the virtual 1000 m seafloor) of  
 426 the 7,652,197 virtual particles released in 2010, for scenario 1 (blue line), 2 (red  
 427 line), 3 (cyan line), and 4 (green line). The cyan rectangle in panel (A) shows  
 428 the region considered for the statistical analyses.

455 from the south and the east of this region, as supported by supplementary anal-  
 456 yses (Supporting Information S.4)

457 The connectivity analysis between the locations where particles left the surface  
 458 and where they reached the seafloor indicated that between 90–95% of the parti-  
 459 cles (scenarios 1–4) deposited at a certain location (defined by a  $\sim 111$  km size  
 460 square) started to sink in other regions (Supporting Information S.3). In the  
 461 Southern Adriatic Sea, where a hotspot of enhanced LDP accumulation was  
 462 identified, between 32–50% of the particles were from adjacent regions. Other  
 463 LDP accumulation regions were detected across the basin, such as in the Tyrre-  
 464 nian and Ionian Seas, in the Strait of Sicily, or in the Eastern Mediterranean.

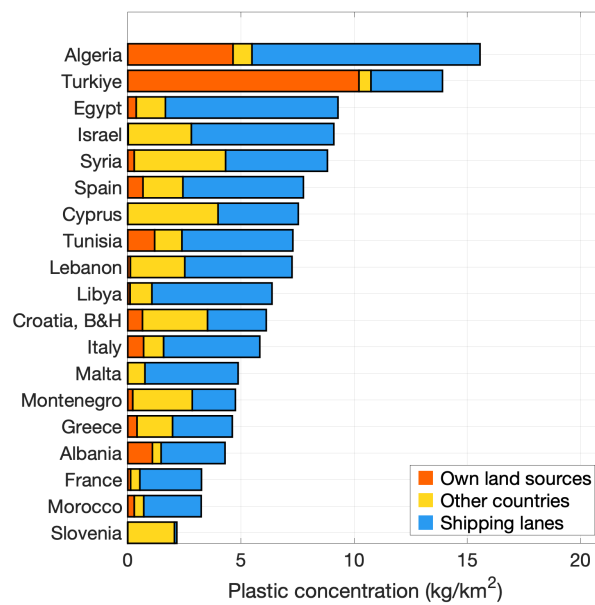
465 The spatial variability between the concentration of virtual LDP particles leav-  
466 ing the surface and reaching the 1000 m virtual seafloor was confirmed also by  
467 the cumulative pdf of the lateral transport distance (Fig. 3F). This was de-  
468 fined as the distance between the locations at which particles left the surface  
469 and those where they reached 1000 m depth. The mean lateral transport dis-  
470 tance for scenario 1 was  $119\pm 99$  km; for scenario 2:  $172\pm 136$  km; for scenario  
471 3:  $232\pm 177$  km; and for scenario 4:  $282\pm 218$  km. The percentage of virtual  
472 LDP particles with a lateral transport distance larger than 100 km was 30%  
473 for scenario 1, increasing to more than 60% for scenario 4. This conclusion was  
474 robust to changes in the horizontal and vertical diffusivity, to the exclusion of  
475 the vertical component of the velocity field, to the increase of the sinking speed  
476 of the LDP particles up to the double of  $SS_{MAX}$ , and to changes of the surface  
477 sinking rate used to initialise the particle starting locations (Supporting Infor-  
478 mation S.6).

479 In situ observations of seafloor plastic concentration in the Mediterranean are  
480 sparse in space and time and differ in methodology. In addition, these collected  
481 all types of plastic, while here we focus on LDP only. Hence, a quantitative  
482 comparison with our model results is currently not possible. Despite these con-  
483 straints, our model predictions qualitatively agree with in situ measurements  
484 (databases and their references in Supporting Information S.7). Largest seafloor  
485 concentrations are reported in the Central Adriatic Sea, close to the Turkiye  
486 shore, and in the Balearic archipelago, where our model predicts the largest  
487 LDP concentrations. Conversely, the lowest concentrations were measured on  
488 the Eastern Sardinia shelf, in the Northern Tyrrhenian Sea, and close to Alicante  
489 (Spain), in agreement with our model predictions (further details in Supporting  
490 Information S.7).

### 491 **3.2 LDP concentration on the coastal strip of Mediter-** 492 **anean countries**

493 The concentration of particles deposited on the coastal strip (i.e. in this study  
494 within 20 km from the coast, Subsec. 2.4) ranged between 5.5–8.9 kg/km<sup>2</sup>  
495 (scenarios 1–4), which was between 11–69% larger than the concentration of  
496 particles sinking from the sea surface above (i.e., less than 20 km from the  
497 coast; 5.2 kg/km<sup>2</sup>). The bottom coastal strips of Algeria and Turkiye showed  
498 the largest particle concentrations (15.6 and 13.9 kg/km<sup>2</sup>, respectively, obtained  
499 from an ensemble average of scenarios 1–4; Fig. 4).

500 We tracked the particles deposited on the bottom coastal strip backward in time  
501 (based on Baudena et al., (31), Methods), and we found that  $\sim 60\%$  were from  
502 vessel discards, while  $\sim 40\%$  were released from land sources. On average,  $\sim 20\%$   
503 of the particles deposited on the coastal strip of a given country were from the  
504 land sources of the same country, while  $\sim 20\%$  were from other countries, with  
505 some variability. For example, 53% of particles deposited on the coastal strip of  
506 Cyprus were from neighbouring countries. The corresponding values for Croatia  
507 and Syria were 47 and 46%, respectively. Conversely, 73% of particles deposited  
508 on the coastal strip of Turkiye were from Turkish coastal sources. Finally,  
509 83% of the particles deposited on the coastal strip of Egypt were from vessel  
510 discards. This proportion was similar for particles deposited on the coastal strip  
511 of Malta and Libya (84 and 83%, respectively). Results obtained for scenarios  
512 1–4 separately (Supporting Information S.8) were consistent with this pattern.



432

433 Figure 4: Concentration of particles released in 2010 which deposited on the  
 434 coastal strip (defined as the region less than 20 km from the coast) of the differ-  
 435 ent Mediterranean countries, obtained from the ensemble average of scenarios  
 436 1–4. For each country, the red rectangle represents the amount of particles de-  
 437 posited on its coastal strip which were released from its own land sources, the  
 438 yellow rectangle represents those released from other countries, and the blue  
 439 rectangle those directly released at sea.



## 513 4 Discussion

### 514 4.1 Pathways and fate of sinking LDP debris

515 The study of the pathways of sinking LDP debris has highlighted that the loca-  
516 tions where LDP debris left the surface did not coincide with the locations where  
517 it was found at depth, as assumed by recent studies (27, 16). This stressed the  
518 importance of a three dimensional approach to study plastic dispersion (69).  
519 When neglecting the vertical component of the currents, the accumulation of  
520 virtual LDP particles in specific regions slightly decreased, e.g. for the area  
521 north-east of the Balearic archipelago (last panel in Fig. S.6). When con-  
522 sidering a virtual seafloor down to 2000 m (Supporting Information S.2), the  
523 accumulation slightly decreased as well. This indicated an important role played  
524 by vertical current shear and by horizontal stirring on the accumulation of LDP  
525 particles, in coherence with recent studies (70, 38). For instance, we observed  
526 a region of LDP particle accumulation at 1000 m depth in the Adriatic Sea.  
527 This matched remarkably well with a recently discovered persistent bottleneck  
528 structure in the circulation of this sea (71), which may be responsible for this  
529 LDP accumulation. In a specific region north-east of the Balearic archipelago,  
530 the number of LDP debris deposited increased for slower sinking speeds. Cross-  
531 roadness analyses indicated a possible mechanism of particle accumulation at  
532 depth (Supporting Information S.4): particles are transported toward this area  
533 due to the regional converging circulation. At the same time, particles sinking  
534 more slowly spend more time suspended in the water column, traveling larger  
535 distances. Hence, the probability they end up in that region increases.  
536 Our simulations also pointed to the fact that a large fraction of LDP particles  
537 could potentially reach the deep sea: 48–63 % of the virtual LDP particles leav-  
538 ing the surface were transported to 1000 m depth, while 38–46 % reached 2000  
539 m in Scenarios 1–3.

540 Even if further information is needed to quantitatively validate our model out-  
541 puts, our results were in general agreement with in situ observations of seafloor  
542 plastic concentration (Supporting Information S.7), corroborating our findings.  
543 In addition, our results were robust with respect to horizontal and vertical dif-  
544 fusivity changes, removal of the vertical velocity current component, variation  
545 of the LDP debris sinking speed, and changes of starting sinking locations (Sup-  
546 porting Information S.6).

### 547 4.2 Bottom coastal LDP pollution.

548 The estimated LDP concentration on the bottom coastal strip increased for  
549 decreasing sinking speeds (from 5.6 kg/km<sup>2</sup> for 7.8 m/d sinking speed to 8.9  
550 kg/km<sup>2</sup> for 1 m/d). This concentration was 11–69% higher than the concentra-  
551 tion of LDP particles leaving the sea surface in the same region (5.2 kg/km<sup>2</sup>).  
552 This indicated that currents at depth tend to propel debris towards coastal re-  
553 gions. This agrees with the pattern of surface currents, which are expected to  
554 retain LDP debris in the majority of Mediterranean coastal regions (27, 31).  
555 Notably, ~ 20% of the particles deposited in the coastal region of a given coun-  
556 try were from neighbouring countries, while ~ 60% were from maritime sources.  
557 The high percentage of deposited LDP debris originating from maritime sources  
558 (60%) is due to the fact that these particles spend more time at the surface

559 than particles released from land sources, which tend to strand quickly and are  
560 therefore less biofouled. In general, while previous studies suggested that each  
561 country is the primary responsible for the plastic pollution of its own beaches  
562 (27, 31), LDP debris on the bottom coastal strip seems to be from multiple  
563 Mediterranean countries and especially from shipping lanes. For instance, Egypt  
564 has been reported to have large rates of beaching plastic debris, mostly released  
565 from its own land sources (27, 31): however, we suggest that its coastal strip  
566 pollution is mainly due to LDP particles released at sea or from other countries.  
567 Overall, LDP pollution emerges as a shared problem in the Mediterranean basin,  
568 as particles polluting the bottom coastal strip were mostly released at sea or  
569 from distant countries.

### 570 **4.3 Implications from comparing the maximum sinking** 571 **speed $SS_{MAX}$ with the sinking speed from a drag model** 572 **$SS_{DM}$**

573 Several biological processes are suspected to affect LDP debris throughout the  
574 water column. Kooi et al., (20) theorised a progressive colonisation of LDP,  
575 which is expected to decrease and eventually cease below the euphotic layer  
576 (due to mineralization or scraping of plastics by copepods; 72). Also, frag-  
577 mentation fosters the slowdown of settling LDP debris, as the vertical sinking  
578 velocity decreases with decreasing debris size (73). Hence, LDP debris may be  
579 resuspended and colonised again (20), as modelled by Lobelle et al., (32), Fischer  
580 et al., (70), and Tsiaras et al., (74). Other biological activities can occur below  
581 the euphotic zone, such as the biofilm formation via heterotrophic organisms  
582 that do not necessarily require light to grow (70). Aggregation in marine snow  
583 and consumption by zooplankton may cause plastic debris to sink, whereas rem-  
584 ineralization at depth would remove organic mass from plastic debris, making it  
585 rise again (75, 76). Zooplankton faecal pellets usually do not reach the seafloor  
586 due to coprophagy (see a review in 77), potentially releasing buoyant plastic  
587 debris. In addition, faecal pellets containing plastic debris are more subject  
588 to fragmentation (25), potentially enhancing resuspension. Chemical processes  
589 can affect the buoyancy of LDP debris as well, especially in regions where bio-  
590 logical activities are limited, such as in the NPGP. For example, weathering of  
591 debris causes hydrogen abstraction with oxygen substitution penetrating deeper  
592 into the polymeric matrix, altering its absolute density (78). Crystallinity also  
593 increases over time during degradative attack of the amorphous regions leading  
594 to an increase in density (79).

595 However, these processes, potentially responsible for the sinking of LDP debris,  
596 have been observed only in laboratory studies or, in situ, uniquely at the sea  
597 surface (21, 22, 23, 24), with the exception of the recent observation of LDP in  
598 marine snow (80). The presence of LDP at depth is hence poorly understood.  
599 To investigate this question, we used a drag model and the largest collection of  
600 Mediterranean LDP debris to date. We calculated the difference of density be-  
601 tween sinking LDP debris and seawater necessary to obtain a theoretical sinking  
602 speed  $SS_{DM}$  equal to  $SS_{MAX}=7.8$  m/d. We obtained  $\Delta\rho=0.025$  kg/m<sup>3</sup>. As  
603 seawater density increases with depth (using a conservative estimate, about 1  
604 kg/m<sup>3</sup> every 100 m; de la Fuente et al., (81)) LDP debris should stop sinking  
605 after 2.5 m if its density does not increase meanwhile. Therefore, our results

606 suggest that the biological processes proposed by the aforementioned studies  
607 (e.g. 20, 75, 76) occur also below the surface.

608 This conclusion is corroborated by the fact that currents, in the Mediterranean  
609 Sea, seems unable to transport LDP debris at great depths. Indeed, Soto-  
610 Navarro et al., (38) have shown that vertical currents redistribute plastic debris  
611 mainly in the first 100 meters of the water column. Onink et al., (82) predicted  
612 a transport to greater depths primarily due to internal tides, but only for a small  
613 proportion of LDP debris (<1%). Tsiaras et al., (74) studied the water column  
614 plastic concentration in some regions of the Mediterranean Sea, and found that  
615 model predictions were orders of magnitude lower than observations. In addition,  
616 de la Fuente et al., (81) argued that neither the vertical nor horizontal  
617 currents affect the water column debris concentration in the Mediterranean Sea  
618 significantly (see in particular their Figure 5). Fischer et al., (70) suggested a  
619 larger impact of vertical transport, but only when associated with an intense  
620 biological activity.

621 All in all, our results point to the fact that LDP debris may persist in the wa-  
622 ter column for time windows larger than previously suspected (e.g. 27, 16) and  
623 travels for hundreds of kilometers. This can increase their bioavailability and  
624 their potential negative impact for marine biota (3, 83). This study provides  
625 an upper limit for the LDP sinking speed that can be used to constrain fu-  
626 ture plastic-tracking studies. Further information on concentration of LDP in  
627 the water column and on the seafloor, as well as observations of in situ sink-  
628 ing speeds are urgently needed, given the potential damage of plastic debris on  
629 pelagic and benthic ecosystems.

#### 630 **4.4 Limits and perspectives**

631 The Lagrangian simulations were subject to approximations. We used a con-  
632 stant sinking velocity of LDP particles from the surface to 1000 m depth, while  
633 this can vary, due to seawater density variation or biochemical processes. The  
634 sinking speed was considered equal for all the particles, while this may not be  
635 the case (Subsec. 2.5). We focused on the 1000 m (and 2000 m, Supporting  
636 Information S.2) depth layer, while several Mediterranean areas are deeper than  
637 3000 m. Particles were released for one year only, and land based and maritime  
638 plastic sources used to calculate the surface sinking rate (our initial condition)  
639 were subject to high uncertainties (12, 27, 31). The surface sinking rate needs  
640 further refinement, including processes such as fragmentation, seasonality and  
641 spatial variability (e.g. 82). The horizontal and vertical diffusivity were consid-  
642 ered as homogeneous through the basin and constant in time, while they can  
643 have both spatial and temporal variability. These choices were due to the fact  
644 that information about concrete ways of parameterising these dynamics (e.g.  
645 the change in time of the sinking speed) were not available or not validated by  
646 observations to date.

647 Therefore, while the concentration of LDPs on the seafloor is affected by high  
648 uncertainties, our results represent a first step forward in the modelisation of  
649 sinking LDP debris, as evidenced also by the agreement with in situ seafloor  
650 observations. The hotspots of plastic debris accumulation on the seafloor as well  
651 as its transport pathways may be used to design optimal sampling or removal  
652 strategies (e.g. 31). These could be focused both at large or regional scales, and  
653 may benefit from future improvements of TrackMPD simulated processes.

654 The previous considerations advocate for further research efforts, as additional  
655 information is essential to deepen the knowledge on the biological processes  
656 affecting the vertical path of plastic debris (e.g. refs. (32, 70, 74, 76)), and  
657 to implement the characterisation of the hydrodynamical field transporting it  
658 (for instance, by increasing its spatio-temporal resolution). Also, resuspension  
659 from the seafloor or funnelling effects (for instance due to canyons) should be  
660 investigated (16, 17, 84). This information is needed to improve plastic-tracking  
661 models and, more generally, to mitigate plastic pollution.

## 662 Supporting Information

663 Use of individual sinking velocities and particle mass; LDP seafloor concentra-  
664 tion at 2000 m; surface-seafloor connectivity; crossroadness analyses; sensitivity  
665 test of  $SS_{DM}$ ; sensitivity test of LDP seafloor concentration; in situ obser-  
666 vations of plastic seafloor concentration; sensitivity test of coastal strip LDP  
667 concentration.

## 668 Acknowledgements

669 We thank the commitment of the following institutions: CNRS, Sorbonne Uni-  
670 versity, LOV. The Tara Ocean Foundation and its founders and sponsors: agnès  
671 b.®, Etienne Bourgois, the Veolia Environment Foundation, Lorient Agglom-  
672 eration, Serge Ferrari, the Foundation Prince Albert II of Monaco, IDEC, the  
673 “Tara” schooner, crews and teams. We thank MERCATOR-CORIOLIS and  
674 ACRI-ST for providing daily satellite data during the expedition. We are also  
675 grateful to the French Ministry of Foreign Affairs for supporting the expedi-  
676 tion and to the countries that graciously granted sampling permission. The  
677 authors are grateful to Enrico Ser-Giacomi for his helpful advice on the de-  
678 sign of the research. We also thank Nicolas Benoit for continuous assistance  
679 on the Mesu computational server, and Thomas Arsouze for the assistance on  
680 the hydrodynamical product used. The authors thank Inés Jambou for her help  
681 with the graphical abstract (Table of Contents graphic). This study is part  
682 of the “PlastiMed BeMed : Closing the plastic tap” project conducted by the  
683 International Union for Conservation of Nature (IUCN) with the financial sup-  
684 port of the Prince Albert II of Monaco Foundation and EU H2020 LABPLAS  
685 project under the grant agreement (ID: 101003954), DOI: 10.3030/101003954.  
686 R.K. furthermore acknowledges support via a Make Our Planet Great Again  
687 grant from the French National Research Agency (ANR) within the Programme  
688 d’Investissements d’Avenir (reference ANR-19-MPGA-0012).

## 689 Data availability

690 All the data necessary to produce all the figures of the main text, including the  
691 LDP seafloor concentration, the coastal strip pollution, and the  $SS_{DM}$  vs  $\Delta\rho$   
692 relationship, are publicly available at <https://doi.org/10.5281/zenodo.7350455>.  
693 The surface sinking rate used to initialise the particle release is available at  
694 <https://doi.org/10.5281/zenodo.5931213>. The in situ plastic concentrations are

<sup>695</sup> available at <https://doi.org/10.5281/zenodo.5538237>. The TrackMPD code is  
<sup>696</sup> available at <https://github.com/IJalonRojas/TrackMPD>.

## References

- 697
- 698 [1] David K. A. Barnes, Francois Galgani, Richard C. Thompson, and Morton  
699 Barlaz, “Accumulation and fragmentation of plastic debris in global envi-  
700 ronments”, *Philosophical Transactions of the Royal Society B: Biological*  
701 *Sciences* **364**(1526), pp. 1985–1998 (2009).
- 702 [2] Nicola J. Beaumont, Margrethe Aanesen, Melanie C. Austen, Tobias Brger,  
703 James R. Clark, Matthew Cole, Tara Hooper, Penelope K. Lindeque, Chris-  
704 tine Pascoe, and Kayleigh J. Wyles, “Global ecological, social and economic  
705 impacts of marine plastic”, *Marine Pollution Bulletin* **142**, pp. 189–195  
706 (2019).
- 707 [3] Susanne Kühn and Jan Andries van Franeker, “Quantitative overview of  
708 marine debris ingested by marine megafauna”, *Marine Pollution Bulletin*  
709 **151**, pp. 110858 (2020).
- 710 [4] José Carlos García-Gómez, Marta Garrigós, and Javier Garrigós, “Plas-  
711 tic as a vector of dispersion for marine species with invasive potential. a  
712 review”, *Frontiers in Ecology and Evolution* **9** (2021).
- 713 [5] Charles Obinwanne Okoye, Charles Izuma Addey, Olayinka Oderinde,  
714 Joseph Onyekwere Okoro, Jean Yves Uwamungu, Chukwudozie Kingsley  
715 Ikechukwu, Emmanuel Sunday Okeke, Onome Ejeromedoghene, and Eli-  
716 jah Chibueze Odii, “Toxic chemicals and persistent organic pollutants as-  
717 sociated with micro-and nanoplastics pollution”, *Chemical Engineering*  
718 *Journal Advances* **11**, pp. 100310 (2022).
- 719 [6] Anthony L. Andrady, “Microplastics in the marine environment”, *Marine*  
720 *Pollution Bulletin* **62**(8), pp. 1596 – 1605 (2011).
- 721 [7] Atsuhiko Isobe, Takafumi Azuma, Muhammad Reza Cordova, Andrés  
722 Cózar, Francois Galgani, Ryuichi Hagita, La Daana Kanhai, Keiri Imai,  
723 Shinsuke Iwasaki, Shin’ichiro Kako, Nikolai Kozlovskii, Amy L. Lusher,  
724 Sherri A. Mason, Yutaka Michida, Takahisa Mituhasi, Yasuhiro Morii,  
725 Tohru Mukai, Anna Popova, Kenichi Shimizu, Tadashi Tokai, Keiichi  
726 Uchida, Mitsuharu Yagi, and Weiwei Zhang, “A multilevel dataset of mi-  
727 croplastic abundance in the world’s upper ocean and the Laurentian Great  
728 Lakes”, *Microplastics and Nanoplastics* **1**(1), pp. 16 (2021).
- 729 [8] Jenna R. Jambeck, Roland Geyer, Chris Wilcox, Theodore R. Siegler,  
730 Miriam Perryman, Anthony Andrady, Ramani Narayan, and Kara Laven-  
731 der Law, “Plastic waste inputs from land into the ocean”, *Science*  
732 **347**(6223), pp. 768–771 (2015).
- 733 [9] Erik Van Sebille, Chris Wilcox, Laurent Lebreton, Nikolai Maximenko,  
734 Britta Denise Hardesty, Jan A Van Franeker, Marcus Eriksen, David Siegel,  
735 Francois Galgani, and Kara Lavender Law, “A global inventory of small  
736 floating plastic debris”, *Environmental Research Letters* **10**(12), pp. 124006  
737 (2015).
- 738 [10] Winnie W. Y. Lau, Yonathan Shiran, Richard M. Bailey, Ed Cook, Mar-  
739 tin R. Stuchtey, Julia Koskella, Costas A. Velis, Linda Godfrey, Julien

- 740 Boucher, Margaret B. Murphy, Richard C. Thompson, Emilia Jankowska,  
741 Arturo Castillo Castillo, Toby D. Pilditch, Ben Dixon, Laura Koerselman,  
742 Edward Kosior, Enzo Favoino, Jutta Gutberlet, Sarah Baulch, Meera E.  
743 Atreya, David Fischer, Kevin K. He, Milan M. Petit, U. Rashid Sumaila,  
744 Emily Neil, Mark V. Bernhofen, Keith Lawrence, and James E. Palardy,  
745 “Evaluating scenarios toward zero plastic pollution”, *Science* **369**(6510),  
746 pp. 1455–1461 (2020).
- 747 [11] Stephanie B. Borrelle, Jeremy Ringma, Kara Lavender Law, Cole C. Mon-  
748 nahan, Laurent Lebreton, Alexis McGivern, Erin Murphy, Jenna Jambeck,  
749 George H. Leonard, Michelle A. Hilleary, Marcus Eriksen, Hugh P. Possing-  
750 ham, Hannah De Frond, Leah R. Gerber, Beth Polidoro, Akbar Tahir, Mi-  
751 randa Bernard, Nicholas Mallos, Megan Barnes, and Chelsea M. Rochman,  
752 “Predicted growth in plastic waste exceeds efforts to mitigate plastic pol-  
753 lution”, *Science* **369**(6510), pp. 1515–1518 (2020).
- 754 [12] Lisa Weiss, Wolfgang Ludwig, Serge Heussner, Miquel Canals, Jean-Francois  
755 Ghiglione, Claude Estournel, Mel Constant, and Philippe Kerhervé, “The  
756 missing ocean plastic sink: Gone with the rivers”, *Science* **373**(6550), pp.  
757 107–111 (2021).
- 758 [13] C. Anela Choy, Bruce H. Robison, Tyler O. Gagne, Benjamin Erwin,  
759 Evan Firl, Rolf U. Halden, J. Andrew Hamilton, Kakani Katija, Susan E.  
760 Lisin, Charles Rolsky, and Kyle S. Van Houtan, “The vertical distribution  
761 and biological transport of marine microplastics across the epipelagic and  
762 mesopelagic water column”, *Scientific Reports* **9**(1), pp. 7843 (2019).
- 763 [14] Matthias Egger, Fatimah Sulu-Gambari, and Laurent Lebreton, “First  
764 evidence of plastic fallout from the North Pacific Garbage Patch”, *Scientific*  
765 *Reports* **10**(1), pp. 7495 (2020).
- 766 [15] Charlotte Lefebvre, Claire Saraux, Olivier Heitz, Antoine Nowaczyk, and  
767 Delphine Bonnet, “Microplastics ftir characterisation and distribution in  
768 the water column and digestive tracts of small pelagic fish in the gulf of  
769 lions”, *Marine Pollution Bulletin* **142**, pp. 510–519 (2019).
- 770 [16] Ian A. Kane, Michael A. Clare, Elda Miramontes, Roy Wogelius, James J.  
771 Rothwell, Pierre Garreau, and Florian Pohl, “Seafloor microplastic  
772 hotspots controlled by deep-sea circulation”, *Science* **368**(6495), pp. 1140–  
773 1145 (2020).
- 774 [17] Martina Pierdomenico, Daniele Casalbore, and Francesco Latino Chiocci,  
775 “Massive benthic litter funnelled to deep sea by flash-flood generated hy-  
776 perpycnal flows”, *Scientific Reports* **9**(1), pp. 5330 (2019).
- 777 [18] F Galgani, J.P Leaute, P Moguedet, A Souplet, Y Verin, A Carpentier,  
778 H Goragner, D Latrouite, B Andral, Y Cadiou, J.C Mahe, J.C Poulard,  
779 and P Nerisson, “Litter on the Sea Floor Along European Coasts”, *Marine*  
780 *Pollution Bulletin* **40**(6), pp. 516 – 527 (2000).
- 781 [19] I. Chubarenko, A. Bagaev, M. Zobkov, and E. Esiukova, “On some physical  
782 and dynamical properties of microplastic particles in marine environment”,  
783 *Marine Pollution Bulletin* **108**(1), pp. 105–112 (2016).

- 784 [20] Merel Kooi, Egbert H. van Nes, Marten Scheffer, and Albert A. Koelmans,  
785 “Ups and downs in the ocean: Effects of biofouling on vertical transport  
786 of microplastics”, *Environmental Science & Technology* **51**(14), pp. 7963–  
787 7971 (2017).
- 788 [21] Francesca M.C. Fazey and Peter G. Ryan, “Biofouling on buoyant marine  
789 plastics: An experimental study into the effect of size on surface longevity”,  
790 *Environmental Pollution* **210**, pp. 354–360 (2016).
- 791 [22] David Kaiser, Nicole Kowalski, and Joanna J Waniek, “Effects of biofouling  
792 on the sinking behavior of microplastics”, *Environmental Research Letters*  
793 **12**(12), pp. 124003 (2017).
- 794 [23] Jan Gerritse, Heather A. Leslie, Caroline A. de Tender, Lisa I. Devriese,  
795 and A. Dick Vethaak, “Fragmentation of plastic objects in a laboratory  
796 seawater microcosm”, *Scientific Reports* **10**(1), pp. 10945 (2020).
- 797 [24] Katerina Karkanorachaki, Evdokia Syranidou, and Nicolas Kalogerakis,  
798 “Sinking characteristics of microplastics in the marine environment”, *Sci-  
799 ence of The Total Environment* **793**, pp. 148526 (2021).
- 800 [25] Matthew Cole, Penelope K. Lindeque, Elaine Fileman, James Clark, Ceri  
801 Lewis, Claudia Halsband, and Tamara S. Galloway, “Microplastics alter the  
802 properties and sinking rates of zooplankton faecal pellets”, *Environmental  
803 Science & Technology* **50**(6), pp. 3239–3246 (2016), PMID: 26905979.
- 804 [26] Adam Porter, Brett P. Lyons, Tamara S. Galloway, and Ceri Lewis, “Role  
805 of marine snows in microplastic fate and bioavailability”, *Environmental  
806 Science & Technology* **52**(12), pp. 7111–7119 (2018), PMID: 29782157.
- 807 [27] S. Liubartseva, G. Coppini, R. Lecci, and E. Clementi, “Tracking plastics  
808 in the Mediterranean: 2D Lagrangian model”, *Marine Pollution Bulletin*  
809 **129**(1), pp. 151 – 162 (2018).
- 810 [28] Maria Luiza Pedrotti, Fabien Lombard, Alberto Baudena, Francois Galgani,  
811 Amanda Elineau, Stephanie Petit, Maryvonne Henry, Romain Troublé,  
812 Gilles Reverdin, Enrico Ser-Giacomi, Mikal Kedzierski, Emmanuel Boss,  
813 and Gabriel Gorsky, “An integrative assessment of the plastic debris load  
814 in the mediterranean sea”, *Science of The Total Environment* **838**, pp.  
815 155958 (2022).
- 816 [29] Mikal Kedzierski, Maiaalen Palazot, Lata Soccalingame, Mathilde Falcou-  
817 Prfol, Gabriel Gorsky, Francois Galgani, Stphane Bruzaud, and Maria Luiza  
818 Pedrotti, “Chemical composition of microplastics floating on the surface  
819 of the Mediterranean Sea”, *Marine Pollution Bulletin* **174**, pp. 113284  
820 (2022).
- 821 [30] Roland Geyer, Jenna R. Jambeck, and Kara Lavender Law, “Production,  
822 use, and fate of all plastics ever made”, *Science Advances* **3**(7) (2017).
- 823 [31] Alberto Baudena, Enrico Ser-Giacomi, Isabel Jalón-Rojas, François Gal-  
824 gani, and Maria Luiza Pedrotti, “The streaming of plastic in the Mediter-  
825 ranean Sea”, *Nature Communications* **13**(1), pp. 2981 (2022).



- 826 [32] Delphine Lobelle, Merel Kooi, Albert A. Koelmans, Charlotte Laufkter,  
827 Cleo E. Jongedijk, Christian Kehl, and Erik van Sebille, “Global modeled  
828 sinking characteristics of biofouled microplastic”, *Journal of Geophysical  
829 Research: Oceans* **126**(4), pp. e2020JC017098 (2021), e2020JC017098  
830 2020JC017098.
- 831 [33] Isabel Jalón-Rojas, Alicia Romero-Ramírez, Kelly Fauquembergue, Linda  
832 Rossignol, Jérme Cachot, Damien Sous, and Bénédicte Morin, “Effects of  
833 biofilms and particle physical properties on the rising and settling velocities  
834 of microplastic fibers and sheets”, *Environmental Science & Technology*  
835 **56**(12), pp. 8114–8123 (2022), PMID: 35593651.
- 836 [34] Andrés Cózar, Marina Sanz-Martín, Elisa Martí, J. Ignacio González-  
837 Gordillo, Bárbara Ubeda, José á. Gálvez, Xabier Irigoien, and Carlos M.  
838 Duarte, “Plastic accumulation in the Mediterranean Sea”, *PLOS ONE*  
839 **10**(4), pp. 1–12 (2015).
- 840 [35] J. Mansui, G. Darmon, T. Ballerini, O. van Canneyt, Y. Ourmieres, and  
841 C. Miaud, “Predicting marine litter accumulation patterns in the mediter-  
842 ranean basin: Spatio-temporal variability and comparison with empirical  
843 data”, *Progress in Oceanography* **182**, pp. 102268 (2020).
- 844 [36] Isabel Jalón-Rojas, Xiao Hua Wang, and Erick Fredj, “A 3D numerical  
845 model to Track Marine Plastic Debris (TrackMPD): Sensitivity of mi-  
846 croplastic trajectories and fates to particle dynamical properties and phys-  
847 ical processes”, *Marine Pollution Bulletin* **141**, pp. 256 – 272 (2019).
- 848 [37] Thomas Arsouze, Jonathan Beuvier, Karine Béranger, Samuel Somot,  
849 C Lebeaupin Brossier, Romain Bourdallé-Badie, and Y Drillet, “Sensi-  
850 bility analysis of the Western Mediterranean Transition inferred by four  
851 companion simulations”, *CIESM, Marseille, France* **27** (2013).
- 852 [38] Javier Soto-Navarro, Gabriel Jordá, Salud Deudero, Carme Alomar, Ángel  
853 Amores, and Montserrat Compa, “3d hotspots of marine litter in the  
854 mediterranean: A modeling study”, *Marine Pollution Bulletin* **155**, pp.  
855 111159 (2020).
- 856 [39] Victor Onink, David Wichmann, Philippe Delandmeter, and Erik van Se-  
857 bille, “The role of Ekman currents, geostrophy, and Stokes drift in the  
858 accumulation of floating microplastic”, *Journal of Geophysical Research:  
859 Oceans* **124**(3), pp. 1474–1490 (2019).
- 860 [40] Kai Liu, Winnie Courtene-Jones, Xiaohui Wang, Zhangyu Song, Nian Wei,  
861 and Daoji Li, “Elucidating the vertical transport of microplastics in the  
862 water column: A review of sampling methodologies and distributions”,  
863 *Water Research* **186**, pp. 116403 (2020).
- 864 [41] G.L. Lattin, C.J. Moore, A.F. Zellers, S.L. Moore, and S.B. Weisberg, “A  
865 comparison of neustonic plastic and zooplankton at different depths near  
866 the southern California shore”, *Marine Pollution Bulletin* **49**(4), pp. 291–  
867 294 (2004).

- 868 [42] Katsiaryna Pabortsava and Richard S. Lampitt, “High concentrations of  
869 plastic hidden beneath the surface of the Atlantic Ocean”, *Nature Com-*  
870 *munications* **11**(1), pp. 4073 (2020).
- 871 [43] Matteo Baini, Maria Cristina Fossi, Matteo Galli, Iliana Caliani, Tommaso  
872 Campani, Maria Grazia Finoia, and Cristina Panti, “Abundance and char-  
873 acterization of microplastics in the coastal waters of tuscany (italy): The  
874 application of the msfd monitoring protocol in the mediterranean sea”,  
875 *Marine Pollution Bulletin* **133**, pp. 543–552 (2018).
- 876 [44] Grigoria Vasilopoulou, George Kehayias, Demetris Kletou, Periklis Kleitou,  
877 Vassilios Triantafyllidis, Anastasios Zotos, Konstantinos Antoniadis, Maria  
878 Rousou, Vassilis Papadopoulos, Polina Polykarpou, and George Tsiamis,  
879 “Microplastics investigation using zooplankton samples from the coasts of  
880 Cyprus (Eastern Mediterranean)”, *Water* **13**(16) (2021).
- 881 [45] Beatriz Rios-Fuster, Montserrat Compa, Carme Alomar, Valentina Fa-  
882 giano, Ana Ventero, Magdalena Iglesias, and Salud Deudero, “Ubiquitous  
883 vertical distribution of microfibers within the upper epipelagic layer of the  
884 western mediterranean sea”, *Estuarine, Coastal and Shelf Science* **266**, pp.  
885 107741 (2022).
- 886 [46] Kai Liu, Feng Zhang, Zhangyu Song, Changxing Zong, Nian Wei, and Daoji  
887 Li, “A novel method enabling the accurate quantification of microplastics  
888 in the water column of deep ocean”, *Marine Pollution Bulletin* **146**, pp.  
889 462–465 (2019).
- 890 [47] Daoji Li, Kai Liu, Changjun Li, Guyu Peng, Anthony L. Andrady, Tianning  
891 Wu, Zhiwei Zhang, Xiaohui Wang, Zhangyu Song, Changxing Zong, Feng  
892 Zhang, Nian Wei, Mengyu Bai, Lixin Zhu, Jiayi Xu, Hui Wu, Lu Wang,  
893 Siyuan Chang, and Wenxi Zhu, “Profiling the vertical transport of mi-  
894 croplastics in the West Pacific Ocean and the East Indian Ocean with a  
895 novel in situ filtration technique”, *Environmental Science & Technology*  
896 **54**(20), pp. 12979–12988 (2020).
- 897 [48] La Daana K. Kanhai, Katarina Grdfeldt, Olga Lyashevskaya, Martin Has-  
898 sellv, Richard C. Thompson, and Ian O’Connor, “Microplastics in sub-  
899 surface waters of the Arctic Central Basin”, *Marine Pollution Bulletin* **130**,  
900 pp. 8–18 (2018).
- 901 [49] X. Peng, M. Chen, S. Chen, S. Dasgupta, H. Xu, K. Ta, M. Du, J. Li,  
902 Z. Guo, and S. Bai, “Microplastics contaminate the deepest part of the  
903 world’s ocean”, *Geochemical Perspectives Letters* **9**, pp. 1–5 (2018).
- 904 [50] A. Bagaev, A. Mizyuk, L. Khatmullina, I. Isachenko, and I. Chubarenko,  
905 “Anthropogenic fibres in the Baltic Sea water column: Field data, labora-  
906 tory and numerical testing of their motion”, *Science of The Total Envi-*  
907 *ronment* **599-600**, pp. 560–571 (2017).
- 908 [51] M R Cordova and U E Hernawan, “Microplastics in Sumba waters, East  
909 Nusa Tenggara”, *IOP Conference Series: Earth and Environmental Science*  
910 **162**, pp. 012023 (2018).

- 911 [52] Elena Gorokhova, “Screening for microplastic particles in plankton sam-  
912 ples: How to integrate marine litter assessment into existing monitoring  
913 programs?”, *Marine Pollution Bulletin* **99**(1), pp. 271–275 (2015).
- 914 [53] Miriam C. Goldstein, Andrew J. Titmus, and Michael Ford, “Scales of spa-  
915 tial heterogeneity of plastic marine debris in the northeast pacific ocean”,  
916 *PLOS ONE* **8**(11), pp. 1–11 (2013).
- 917 [54] M.B. Zobkov, E.E. Esiukova, A.Y. Zyubin, and I.G. Samusev, “Microplas-  
918 tic content variation in water column: The observations employing a novel  
919 sampling tool in stratified Baltic Sea”, *Marine Pollution Bulletin* **138**, pp.  
920 193–205 (2019).
- 921 [55] Young Kyoung Song, Sang Hee Hong, Soeun Eo, Mi Jang, Gi Myung Han,  
922 Atsuhiko Isobe, and Won Joon Shim, “Horizontal and Vertical Distribution  
923 of Microplastics in Korean Coastal Waters”, *Environmental Science &  
924 Technology* **52**(21), pp. 12188–12197 (2018).
- 925 [56] Mine B. Tekman, Claudia Wekerle, Claudia Lorenz, Sebastian Pimpke,  
926 Christiane Hasemann, Gunnar Gerdt, and Melanie Bergmann, “Tying up  
927 loose ends of microplastic pollution in the Arctic: Distribution from the  
928 sea surface through the water column to deep-sea sediments at the HAUS-  
929 GARTEN Observatory”, *Environmental Science & Technology* **54**(7), pp.  
930 4079–4090 (2020), PMID: 32142614.
- 931 [57] Shiye Zhao, Erik R. Zettler, Ryan P. Bos, Peigen Lin, Linda A. Amaral-  
932 Zettler, and Tracy J. Mincer, “Large quantities of small microplastics  
933 permeate the surface ocean to abyssal depths in the south atlantic gyre”,  
934 *Global Change Biology* **28**(9), pp. 2991–3006 (2022).
- 935 [58] Mikael L. A. Kaandorp, Henk A. Dijkstra, and Erik van Sebille, “Closing  
936 the Mediterranean marine floating plastic mass budget: Inverse modeling  
937 of sources and sinks”, *Environmental Science & Technology* **54**(19), pp.  
938 11980–11989 (2020), PMID: 32852202.
- 939 [59] Julien Boucher and Guillaume Billard, “The mediterranean: Mare plas-  
940 ticum”, *Gland, Switzerland: IUCN. x* **62** (2020).
- 941 [60] Mita Drius, Lucia Bongiorno, Daniel Depellegrin, Stefano Menegon,  
942 Alessandra Pugnetti, and Simon Stifter, “Tackling challenges for Mediter-  
943 ranean sustainable coastal tourism: An ecosystem service perspective”,  
944 *Science of The Total Environment* **652**, pp. 1302–1317 (2019).
- 945 [61] Beatriz Morales-Nin, Antoni M. Grau, and Miquel Palmer, “Managing  
946 coastal zone fisheries: A Mediterranean case study”, *Ocean & Coastal  
947 Management* **53**(3), pp. 99–106 (2010).
- 948 [62] AJ Florczyk, M Melchiorri, C Corbane, M Schiavina, M Maffenini, M Pe-  
949 saresi, P Politis, S Sabo, S Freire, D Ehrlich, T Kemper, P Tommasi,  
950 D Airaghi, and L Zanchetta, “Description of the GHS Urban Centre  
951 Database 2015”, *GHS Urban Centre Database 2015, multitemporal and  
952 multidimensional attributes. European Commission, Joint Research Centre  
953 (JRC)* (2019).

- 954 [63] Laurent C. M. Lebreton, Joost van der Zwet, Jan-Willem Damsteeg, Boyan  
955 Slat, Anthony Andrady, and Julia Reisser, “River plastic emissions to the  
956 world’s oceans”, *Nature Communications* **8**(1), pp. 15611 (2017).
- 957 [64] Lin Wu, Yongjun Xu, Qi Wang, Fei Wang, and Zhiwei Xu, “Mapping  
958 global shipping density from AIS Data”, *Journal of Navigation* **70**(1), pp.  
959 6781 (2017).
- 960 [65] Enrico Ser-Giacomi, Vincent Rossi, Cristóbal López, and Emilio  
961 Hernández-García, “Flow networks: A characterization of geophysical  
962 fluid transport”, *Chaos: An Interdisciplinary Journal of Nonlinear Sci-  
963 ence* **25**(3), pp. 036404 (2015).
- 964 [66] Alberto Baudena, Enrico Ser-Giacomi, Cristóbal López, Emilio Hernández-  
965 García, and Francesco d’Ovidio, “Crossroads of the mesoscale circulation”,  
966 *Journal of Marine Systems* **192**, pp. 1 – 14 (2019).
- 967 [67] F. Dioguardi, D. Mele, and P. Dellino, “A new one-equation model of fluid  
968 drag for irregularly shaped particles valid over a wide range of reynolds  
969 number”, *Journal of Geophysical Research: Solid Earth* **123**(1), pp. 144–  
970 156 (2018).
- 971 [68] Michiel Van Melkebeke, Colin Janssen, and Steven De Meester, “Character-  
972 istics and sinking behavior of typical microplastics including the potential  
973 effect of biofouling: Implications for remediation”, *Environmental Science  
974 & Technology* **54**(14), pp. 8668–8680 (2020), PMID: 32551546.
- 975 [69] I. Jalón-Rojas, X.-H. Wang, and E. Fredj, “Technical note: On the im-  
976 portance of a three-dimensional approach for modelling the transport of  
977 neustic microplastics”, *Ocean Science* **15**(3), pp. 717–724 (2019).
- 978 [70] R. Fischer, D. Lobelle, M. Kooi, A. Koelmans, V. Onink, C. Laufkötter,  
979 L. Amaral-Zettler, A. Yool, and E. van Sebille, “Modeling submerged bio-  
980 fouled microplastics and their vertical trajectories”, *Biogeosciences Dis-  
981 cussions* **2021**, pp. 1–29 (2021).
- 982 [71] Enrico Ser-Giacomi, Alberto Baudena, Vincent Rossi, Mick Follows, Sophie  
983 Clayton, Ruggero Vasile, Cristóbal López, and Emilio Hernández-García,  
984 “Lagrangian betweenness as a measure of bottlenecks in dynamical systems  
985 with oceanographic examples”, *Nature Communications* **12**(1), pp. 4935  
986 (2021).
- 987 [72] Julia Reisser, Maira Proietti, Jeremy Shaw, and Charitha Pattiaratchi,  
988 “Ingestion of plastics at sea: does debris size really matter?”, *Frontiers in  
989 Marine Science* **1** (2014).
- 990 [73] Amanda L. Dawson, So Kawaguchi, Catherine K. King, Kathy A.  
991 Townsend, Robert King, Wilhelmina M. Huston, and Susan M. Bengt-  
992 son Nash, “Turning microplastics into nanoplastics through digestive frag-  
993 mentation by antarctic krill”, *Nature Communications* **9**(1), pp. 1001  
994 (2018).

- 995 [74] Kostas Tsiaras, Yannis Hatzonikolakis, Sofia Kalaroni, Annika Pollani, and  
996 George Triantafyllou, “Modeling the pathways and accumulation patterns  
997 of micro- and macro-plastics in the Mediterranean”, *Frontiers in Marine  
998 Science* **8** (2021).
- 999 [75] Karin F. Kvale, A. E. Friederike Prowe, and Andreas Oschlies, “A critical  
1000 examination of the role of marine snow and zooplankton fecal pellets in  
1001 removing ocean surface microplastic”, *Frontiers in Marine Science* **6**, pp.  
1002 808 (2020).
- 1003 [76] K. Kvale, A. E. F. Prowe, C.-T. Chien, A. Landolfi, and A. Oschlies, “The  
1004 global biological microplastic particle sink”, *Scientific Reports* **10**(1), pp.  
1005 16670 (2020).
- 1006 [77] Jefferson T. Turner, “Zooplankton fecal pellets, marine snow, phytodetritus  
1007 and the oceans biological pump”, *Progress in Oceanography* **130**, pp. 205–  
1008 248 (2015).
- 1009 [78] Annika Jahnke, Hans Peter H. Arp, Beate I. Escher, Berit Gewert,  
1010 Elena Gorokhova, Dana Khnel, Martin Ogonowski, Annegret Pothoff,  
1011 Christoph Rummel, Mechthild Schmitt-Jansen, Erik Toorman, and  
1012 Matthew MacLeod, “Reducing uncertainty and confronting ignorance  
1013 about the possible impacts of weathering plastic in the marine environ-  
1014 ment”, *Environmental Science & Technology Letters* **4**(3), pp. 85–90 (2017).
- 1015 [79] M. J. Jenkins and K. L. Harrison, “The effect of crystalline morphology  
1016 on the degradation of polycaprolactone in a solution of phosphate buffer  
1017 and lipase”, *Polymers for Advanced Technologies* **19**(12), pp. 1901–1906  
1018 (2008).
- 1019 [80] Luisa Galgani, Isabel Gomann, Barbara Scholz-Bttcher, Xiangtao Jiang,  
1020 Zhanfei Liu, Lindsay Scheidemann, Cathleen Schlundt, and Anja Engel,  
1021 “Hitchhiking into the Deep: How Microplastic Particles are Exported  
1022 through the Biological Carbon Pump in the North Atlantic Ocean”, *Envi-  
1023 ronmental Science & Technology* **0**(0), pp. null (2022), PMID: 36302504.
- 1024 [81] R. de la Fuente, G. Drótos, E. Hernández-García, C. López, and E. van  
1025 Sebille, “Sinking microplastics in the water column: simulations in the  
1026 Mediterranean Sea”, *Ocean Science* **17**(2), pp. 431–453 (2021).
- 1027 [82] Victor Onink, Mikael L. A. Kaandorp, Erik van Sebille, and Charlotte  
1028 Laufketter, “Influence of Particle Size and Fragmentation on Large-Scale  
1029 Microplastic Transport in the Mediterranean Sea”, *Environmental Science  
1030 & Technology* **0**(0), pp. null (2022), PMID: 36270631.
- 1031 [83] S. Fabri-Ruiz, A. Baudena, F. Moulec, F. Lombard, J.-O. Irisson, and M.L.  
1032 Pedrotti, “Mistaking plastic for zooplankton: Risk assessment of plastic  
1033 ingestion in the mediterranean sea”, *Science of The Total Environment*  
1034 **856**, pp. 159011 (2023).
- 1035 [84] A. Ballent, S. Pando, A. Purser, M. F. Juliano, and L. Thomsen, “Modelled  
1036 transport of benthic marine microplastic pollution in the Nazaré Canyon”,  
1037 *Biogeosciences* **10**(12), pp. 7957–7970 (2013).